THE REVIEW OF PHYSICAL CHEMISTRY OF JAPAN, VOL. 50, 1980

VISCOSITIES AND GLASS TRANSITIONS IN LIQUIDS AT HIGH PRESSURES

By R. G. Munro, G. J. Piermarini, and S. Block

The study of the pressure dependence of the viscous properties of liquids, including glass transitions, is reviewed. An overview of the present status of both the theory of viscosity and the experimental techniques and results for high pressure viscometry is presented. Representative examples of several viscometers for high pressure applications are described briefly. A more detailed description of the diamond anvil pressure cell falling sphere viscometer is given. Viscosity data obtained by this method for several liquids are correlated with their glass transition pressures which are derived from ruby fluorescence line-broadening measurements.

1. Introduction

The subject of viscosity has been pursued for approximately three hundred years, and glass transitions have been studied for about sixty years. During that time, these topics have been both fruitful and frustrating. The many studies have produced much information about the microscopic structure of fluids, the intermolecular potentials, and the dynamics of intermolecular interactions and rate processes. The results have been important to such diverse applications as lubrication technology, geology, rheology, physiology, and astrogeophysics. In fact, the results of the study of viscosity are pertinent to all physical problems or applications involving the flow of a substance.

Throughout most of the history of this subject, the temperature dependence of the coefficient of viscosity has been at the center of attention. The reason for this circumstance is essentially technical: The temperature variable was relatively easy to control and sustain at an early stage in the development of the science. It is only in relatively recent times that a wide range of very large static pressure has been routinely accessible in viscometry. As the high pressure devices have been developed, there has been a corresponding growth in the interest in the pressure dependence of liquid viscosity and in the related phenomenon of the glass transition. Part of this interest is due to the fact that volume changes obtained by means of modest pressure increments tend to be much larger than the volume changes obtainable by means of temperature variations. Furthermore, the influence of temperature is complicated by statistical and kinetic effects. As a result, pressure variations can be more effective than

(*Received August 26, 1980*)

The Review of Physical Chemistry of Japan Vol. 50 (1980)

temperature variations for investigating the relationship between transport properties and the intermolecular potentials which are inherently distance-dependent.

The development of high pressure devices has produced its own additional interest in viscosity. Obviously, it is most desirable to conduct measurements of the pressure dependence of any material's property in an environment with a well defined hydrostatic pressure. For this purpose, liquids rather than solids are used as pressure transmitting media. Since viscosity is a measure of the resistance to shear, the effectiveness of a given liquid as a pressure medium varies with the magnitude of its viscosity. Of particular interest is the identification of the region of temperature and pressure within which the liquid transforms to the glassy state.

The review is concerned generally with the viscous properties of liquids at high pressure. The term "high pressure" is a relative one which has different quantitative meanings in different contexts. Presently, there appears to be a natural division of the high pressure viscometry of liquids into two groups according to the designed pressure capacities of the viscometers: those which operate with pressure $P \lesssim 2$ GPa and those which operate beyond 2 GPa. In the latter case, the pressure capabilities of the viscometers usually exceed the glass transition pressures of the liquids.

The following sections begin with a survey of the present theoretical understanding of liquid viscosity. Several high pressure viscometers which are representative of the field are then described briefly. This is followed by a detailed discussion of the latest development in high pressure viscometry (from the point of view of the largest accessible pressure range): the diamond anvil falling sphere viscometer. The ruby method of pressure measurement and its use as a means of detecting the glass transition in liquids is also described. Utilizing viscosity data and glass transition pressures which are obtained by the diamond cell and ruby pressure measurement methods, a model is proposed to correlate and characterize the pressure dependence of viscosity at high pressure with the glass transition pressure.

2. Current Theories

The coefficient of viscosity for any material is a measure of that material's resistance to shear forces and incorporates common characteristics of continuum fluids. The first of these is that the material can flow in response to an applied shear stress. The second is that the fluid has a dissipative resistance to flow. Hence, the viscosity coefficient is a measure of a bulk property of the material which assumes the presence of a velocity gradient. In the Newtonian picture of fluids, the steady state consists of laminar flow, and a viscous force is manifested by the transport of momentum between successive layers of the fluid.

In the extreme case of very dilute gases, the primary means by which momentum transport occurs is the actual migration of atoms from one layer of the substance to another. In other words, for these substances, the mean free path of motion is relatively large. As the density of the gas increases, however, the interactions among the particles also increase, and the

The Review of Physical Chemistry of Japan Vol. 50 (1980)

momentum transport becomes increasingly dependent on the interatomic forces as well as the velocity distribution. For gases, the translational motion remains the dominant contribution to the momentum transport, and indeed, because of this, Lennard-Jones[1] was able to investigate the force laws for several atoms by means of the theory of the viscosity of gases.

The situation changes when the atoms condense to form a liquid. In the liquid phase the atoms are always within the range of significant interatomic interactions. Consequently, the atoms can no longer be considered, at any time, as individually free, or nearly free, with respect to translational motion. Instead, interatomically coupled reorientational and vibrational motions and molecular distortions must be given more detailed consideration. This strong dependency of the viscosity of a liquid, a bulk, nonequilibrium property, on the interatomic potential makes the problem of the viscosity of liquids far more complicated than it is for gases, and while kinetic theory is acknowledged as satisfactory for gases, no comparably successful theory has been found for liquids. One result of this circumstance has been a plethora of empirical relations which are used to describe viscosity as a function of temperature and/or pressure or density. All of these expressions (which number more than 30) are lacking in mathematical rigor and have limited ranges of applicability. However, it can be said that some of the models are much more attentive to microscopic details than are others. Advanced models of the liquid state which are especially to be noted include the free volume theory,[2-5] the entropy theory[6-8] and the significant structure theory.[9-11]

It is ptossible to obtain mathematical rigor in the context of the fluctaution dissipation theory which provides formal expression for transport properties for both Newtonian and non-Newtonian liquids while utilizing the formalism of equilibrium statistical mechanics. The basic idea in this approach is that an equilibrium system undergoes statistical fluctuations from its equilibrium state, and necessarily the return to equilibrium involves the transport properties of the system. According to the fluctuation-dissipation theory, the shear viscosity of a liquid is determined by means of the autocorrelation function of any off-diagonal component of the stress tensor. Unfortunately, at this point, the mathematical complexities of the problem usually require the introduction of model approximations. Consequently, detailed analyses have been limited to very simple systems such as those described by hard sphere[12-14] and square well[15-17] potentials. A comprehensively useful theory of liquid viscosity for all ranges of pressure and temperature has yet to be achieved.

3. High Pressure Viscometry

The designs of the high pressure viscometers reviewed here generally have been of the types labeled: capillary, rolling ball, falling ball, falling cylinder, concentric cylinder, swinging vane, and vibrating crystal. During the past one hundred years, these methods have been used to investigate the pressure dependence of viscosity with varying degrees of success and over various ranges of pressure and temperature. Roentgen[18] appears to have been the first to have used a

capillary flow viscometer to give the first report on the pressure dependence of the viscosity of water. He reported a one percent change in viscosity for a pressure of about 0.002 GPa. Among the few early works that followed this report, the most remarkable is probably that of Barus[19] who undertook an extensive study of marine glue and gave results for pressures up to about 0.2 GPa, a two order increase in the magnitude of pressure. Much of the work following these initiations has been centered upon the attainment of technical advances in the pressure apparatus and the measurement techniques.

3-1. Pressure Less than 2 GPa

The falling ball viscometer of Kuss[20] has recently been modified to accomodate pressures to 0.4 GPa and temperatures to 300°C. This represents a doubling of the previous pressure range of the device and a quadrupling of its temperature range. The viscosity is determined by electronically measuring the time of descent of the falling ball. Results with an accuracy of adout 0.5% were reported for temperatures up to 200°C and pressures up to 0.25 GPa for poly-isobutene, white oil, and a commercial mineral oil.

A falling cylinder viscometer (Fig. 1) was used by Tanaka *et al.*[21] to determine the specific volume and viscosity of ethanol-water mixtures. Their apparatus can generate pressures up to about 0.3 GPa, and it can be used at various temperatures. Viscosity data with an accuracy of ±2% were given for mixtures at 25°C and 50°C with pressures up to about 0.1 GPa. In later work by this group, Kubota *et al.*[22] used the same apparatus to make measurements on methanol-water mixtures over the temperature range 10-75°C.

In their study of lubricating fluids, Hutton and Phillips[23] have constructed a concentric cylinder viscometer in which the inner cylinder is rotated. The viscous drag of the test liquid transmits a torque to the stationary (outer) cylinder which is equipped with strain gauges.

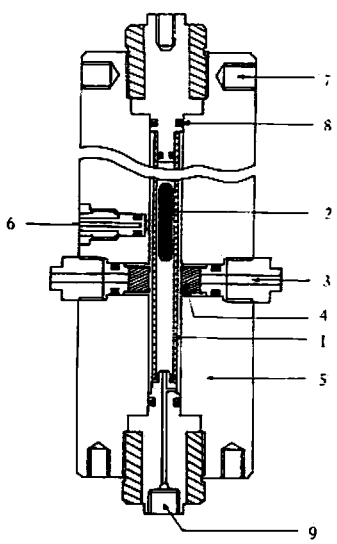

Fig. 1. Schematic diagram of the falling-cylinder viscometer employed by Tanaka *et. al.*[21] The apparatus consits of a precisely bored Pyrex glass tube [1] mounted coaxially in a high pressure vessel, [5], and a glass cylindrical, plummet [2] with hemispherical ends. The falling time of the cylinder is determined within ±0.1 ms utilizing an electronic time-interval counter, a He-Ne gas laser beam [3] passed through a pair of optical windows [4] and a phototransitor. To return the plummet to its starting position, the viscometer can be rotated on a horizontal axis. Temperature can be maintained constant to within 0.05°C and is measured with a thermistor [6] device. The mean reproducibility of the falling time was 0.5%. Due to unknown geometric and wall effects, the apparatus needs to be calibrated with a fluid of known viscosity.

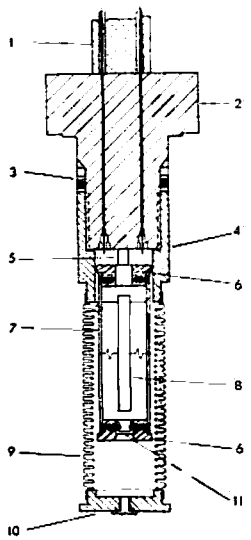

Fig. 2. Cross-section diagram of the crystal assembly attached to the pressure vessel closure [2] developed by Collings and McLaughlin.[24] The quartz crystal [8] is surrounded by the test liquid, both of which are separated from the hydraulic fluid by a stainless steel sleeve [4] and a stainless steel bellows [9], which allows compression. The system is designed for 1 GPa. The viscosity is related to the damping effect of the viscous medium on the torsionally vibrating quartz crystal.

Measurement of the strain as a function of the rotational speed of the inner cylinder determines the viscosity by comparison with the results for a calibrant substance. The accessible pressure range is about 0.5 GPa with a reported accuracy in the viscosity measurement of about 5-10%, depending on the magnitude of the viscosity. Results are given for polyphenyl ether to 0.25 GPa.

A viscometer (Fig. 2), in which a vibrating quartz crystal is used to determine viscosity at pressures up to 1 GPa for temperatures up to 100°C has been developed by Collings and McLaughlin.[24] Because of the viscous damping of the fluid, there is a change in the resonant frequency and the crystal resistance at resonance. From the known relation of these changes to the viscosity and density of the liquid, results with an estimated accuracy of 0.5% were presented for benzene, cyclohexane, carbon tetrachloride, isopentane, and *n*-pentane.

Another example of the popular falling cylinder viscometer is provided by the work of Dickinson.[25] This device, calibrated at atmospheric pressure using hydrocarbons and alcohols, can be operated up to about 0.5 GPa. The temperature of the viscometer is controlled by immersing the apparatus in an oil bath in which temperature is maintained to ±0.1K. Results were presented for *n*-hexane, *n*-octane, hexamethyldisiloxane, octamethylcyclotrtesiloxane, and mixtures of these substances.

One of the earliest viscometers in this class also achieved some of the highest pressures. This was Bridgman's[26] falling cylindrical weight device. With this viscometer (Fig. 3), pressures up to about 1.2 GPa were generated, and the results for 43 liquids were presented for temperatures of 30°C and 75°C.

More recently, Irving and Barlow[27] constructed an automated falling cylinder viscometer which can be operated at pressures up to about 1.4 GPa. Their report included results for di-(*n*-butyl) phthalate and di-(2-ethylhexyl) phthalate at 30°C with an estimated accuracy of ±2%.

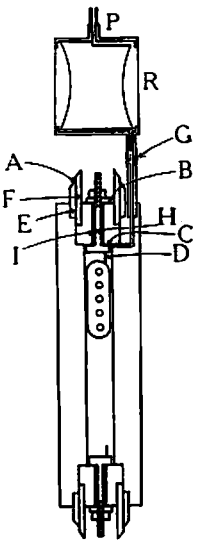

Fig. 3. A cross-section diagram of the falling-cylinder viscometer used by Bridgman.[26] A steel cylinder is filled with the test liquid. A steel cylindrical weight with hemispherical surfaces at both ends (indicated by the region designated by small open circles) and separated from the walls of the cylinder by a narrow annulus through the liquid in the cylinder by gravity. The time of vertica fall of the weight from one end of the cylinder to the other is measured electrically. The viscosity is proportional to this measured time of fall. The interesting feature of this system is the electrically insulated terminal (D) at both ends of the cylinder against which the weight rests at the end of its fall. In this position, electrical connection is made which activates a suitable timing device. The entire cylindrical apparatus can be rotated 180° on a horizontal axis to permit reversal of the system and the time of fall can be determined in the opposite direction.

3-2. Pressure Greater than 2 GPa

Bridgman[28] led the way to higher pressures with the development of a swinging vane viscometer, (Fig. 4), which was capable of reaching pressures of about 4 GPa. He used this apparatus to extend his previous measurements on pure liquids and to study polymers and commercial liquids. The extension of viscometry to greater pressure presented considerable difficulty because of the small volumes required for the successful generation of the pressures.

A cylindrical plunger with tapered ends was used by Zilberstein and Dill[29] in their construction of a falling weight viscometer. Their device can operate at pressures up to 3 GPa and temperatures up to 200°C. They obtained results for hydraulic oil (HO-1), white gasoline, a 1-1 mixture of the oil and gasoline, and a synthetic commercial fluid. Their

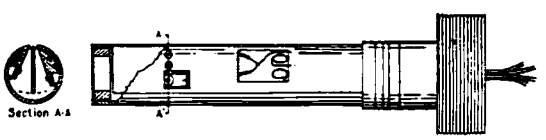

Fig. 4. Cross-section of the swinging-vane apparatus for measuring viscosity developed by Bridgman.[26] The apparatus does not give absolute viscosity, but does give the relative viscosity. The falling member, in this case, is a vane pivoted about an offset longitudinal axis. The vane rotates 60° between stops (section A-A') which are electrically insulated and at the same time provides electrical contact so that the time of rotation of the vane can be measured electrically. By varying the thickness of the vane, the fall-time can be varied. For liquids of high viscosity, the vane was replaced by a gold bar. The total range of viscosity observed in this apparatus for isopropyl alcohol for example, varied one million fold.

measurements went to 2.5 GPa and 150°C with an accuracy of ±5%.

A variation of the falling ball viscometer is used in the study of the viscosity of high temperature melts at high pressure. The work of Kushiro[30,31] is representative of this method. Initially, the ball is placed on the top of the solid sample. The sample is then heated to melting, and the ball falls. After a time on the order of minutes, the temperature of the sample is quenched causing the sample to solidify thereby freezing the ball at its final depth which can then be measured. A plot of distance against time yields the terminal velocity, and Stokes formula determines the viscosity. Melts at temperatures of about 1400°C with pressures up to about 3 GPa have been studied.

The first report of results beyond the pressure limit established by Bridgman in 1949 was made by Barnett and Bosco.[32] Their design returned to the capillary type of viscometer (Fig. 5), and with it, they were able to achieve pressures to 6 GPa. They reported viscosities at room temperature for petroleum ether, 1 : 1 *n*-pentane and isopentane, and isopropyl alcohol.

The viscometer which can operate at the highest pressures was introduced by Piermarini, Forman, and Block.[33] It is of the falling ball type and utilizes a diamond anvil pressure cell (DAPC). Since the DAPC can achieve pressures far in excess of the glass transition pressure of any normal liquid, the principal limitation of this viscometer is not pressure but the time required for the ball to traverse the cell. Measurements have been made on 4 : 1 methanol-ethanol to 7 GPa and on *n*-butyl chloride to 3.6 GPa at room temperature.

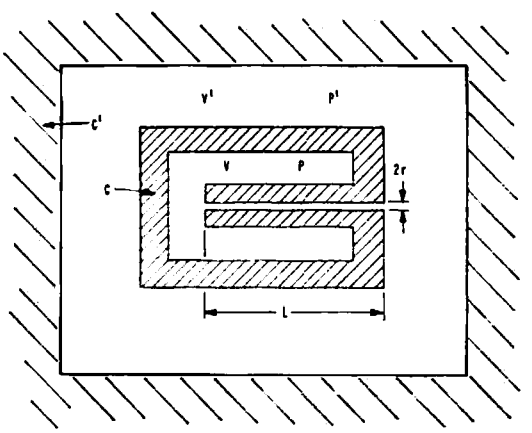

Fig. 5. Diagrammatic cross-section of the cylindrical capillary-type viscometer developed by Barnett and Bosco[32] for measurements up to 6 Gpa. The basic principal of the apparatus is as follows. Two cylindrical chambers C and C′ with enclosed volumes V and V′ are connected by a capillary tube of length L and radius r. By means of an applied external pressure P', a time-dependent pressure difference $(P'-P>0)$ exists between the ends of the capillary tube. This pressure difference results in viscous flow, and the subsequent equilibration time can be related to the viscosity of the test liquid. At equilibrium, there can be no pressure difference between the two volumes $(P'-P=0)$ and therefore no viscous flow.

4. Diamond Anvil Pressure Cell Falling Sphere Viscometer

This section considers the use of a diamond cell as a falling sphere viscometer. A discussion of the associated measurement apparatus is included, but greater detail can be found in the previously published descriptions.[34-36]

The essential component of a diamond cell is the anvil assembly, an enlarged cross-sectional drawing of which is shown in Fig. 6. Diamonds with anvil faces ranging between 0.25 and 0.75 mm^2 in area are used in an opposed gasketed configuration. Inconel metal sheets approximately 0.25 mm in thickness containing a hole as large as 0.5 mm in diameter are used to confine the liquid between the two diamond anvils. These dimensions are initial values and it should be noted that with increasing pressure the dimensions decrease to produce a decrease in volume.

A solid Ni alloy sphere (0.035 mm diameter) is confined in the gasket hole containing the liquid along with a small chip of ruby, approximately the same size as the Ni sphere, which is the pressure sensor.

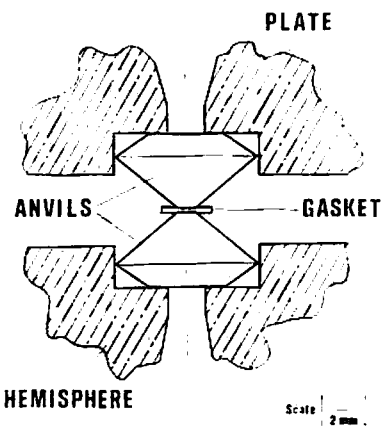

Fig. 6. Enlarged cross-section drawing of the opposed diamond anvil configuration showing details of the anvil shape, their loadbearing metal supports and the metal gasket confining the liquid sample.

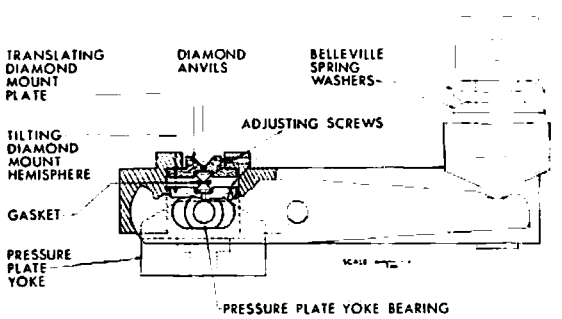

Fig. 7. Cut-away cross-section drawing of the ultrahigh pressure diamond cell used as a falling sphere viscometer. The essential components include the anvil supports, alignment features, lever-arm assembly and spring washer loading system.

In the NBS design, (Fig. 7), the force is produced by compressing Belleville spring washers by the simple rotation of the large screw. The spring lever-arm arrangement generates a uniform and continuously varying force as the screw is rotated. Furthermore, the sensitivity and magnitude of the load can be varied, by using the spring washers either in series or in parallel as desired.

Through the lever-arm assembly the force is magnified by a factor of 2 and is applied directly to the anvil mounted in the extended piston *via* the pressure plate. The opposing anvil is fixed in position and acts as an entablature. To avoid diamond anvil failure under load, facility for aligning the anvil faces both axially and horizontally is provided by the tilting feature in the hemisphere and the translation capability in the entablature plate. The cell shown here is fabricated* from Vascomax 300, heat treated to a hardness of RWC 52-55. The translation plate and the hemisphere, however, are fabricated from 4340 alloy steel hardened to RWC 59-60 to prevent indentation by the tables of the diamond anvils when under large applied loads. Since the diamonds are transparent they are also used as optical windows in order to view the liquid sample, the falling Ni sphere and the ruby chip as shown in Fig. 8.

The assembled pressure cell is mounted on a modified optical goniometer as shown in the photograph in Fig. 9. The translational motions of the goniometer are used to position and to focus the pressure cell in relation to a microscope which is used for viewing the Ni sphere as it falls through a liquid under pressure. The rotational feature of the goniometer permits rapid inversion of the cell while maintaining optical alignment. The position of the sphere falling under the action of gravity can be determined accurately as a function of time by utilizing the calibrated distance scale which is contained in the eye piece of the microscope. (See Fig. 8) Thus its velocity at any time can be computed. The image of the sample and a digital clock can also be displayed on a TV monitor as well as recorded on video tape for future reference.

Pressure is measured by an optical fluorescence system which utilizes the pressure dependent shift of the R_1 ruby fluorescence line at 6942A.[36] The pressure dependence was calibrated against the compression of NaCl and was found to be linear (0.365A/kbar) up to

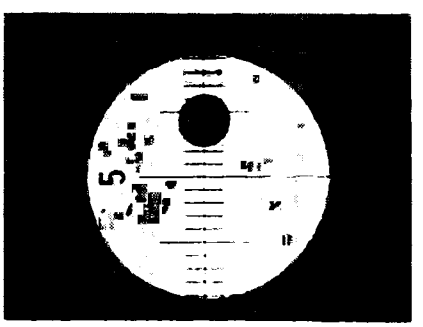

Fig. 8. A view of the solid Ni sphere falling through the Dow-Corning 200 fluid in a gravitational field. The smallest graduation on the superimposed graduated scale for the particular optics used is 0.0095 mm.

* Use of trade names in this paper does not imply endorsement by the National Bureau of Standards.

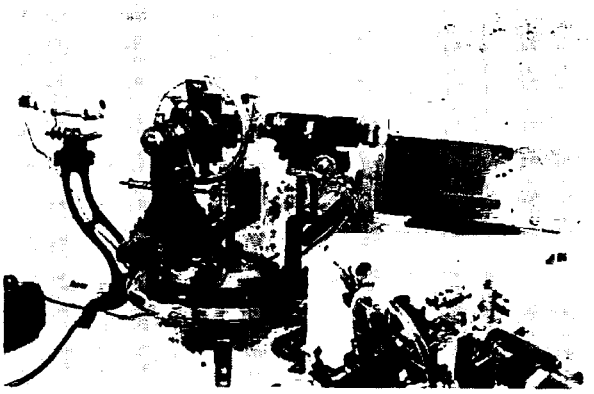

Fig. 9. A photograph of the viscosity measurement system showing the diamond pressure cell mounted on a modified optical goniometer. A stationary microscope attached to the goniometer permits viewing the sample through the diamond windows of the pressure cell.

29.0 GPa with pressures derived from the Decker equation of state of NaCl.[37]

In practice a small chip of crystalline ruby (0.5% Cr) is placed in the cell along with the Ni sphere and the liquid where viscosity is to be measured. The ruby fragment generally does not interfere significantly with the velocity measurement, and, in cases where this condition is not met, ruby spheres have been substituted for the Ni sphere which permits both a pressure measurement and a velocity measurement from the same object.

Not only is the energy of the ruby fluorescent *R* lines pressure dependent (Fig. 10) but the line-shape is also.[38] The line-shape is particularly sensitive to nonuniform shear stresses and this property has been used to determine the glass transition pressure of liquids as shown in Fig. 11. Large increases in line-width are observed above the glass transition pressure, and this effect has been attributed to the shear stresses which are supported by the glassy medium. The pressure dependence of viscosity and the onset of the glassy state are related, and, as we

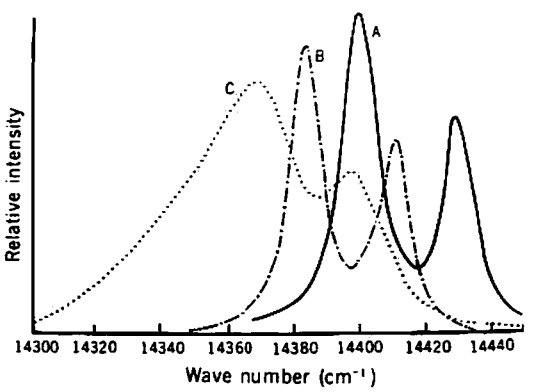

Fig. 10. The R-line luminescence spectra of a crystal of ruby in the diamond cell: Curve A, ruby sample at ambient atmospheric pressure; Curve B, ruby sample at approximately 2.26 GPa hydrostatic pressure; and Curve C, ruby sample at approximately 4.0 GPa nonhydrostatic pressure.

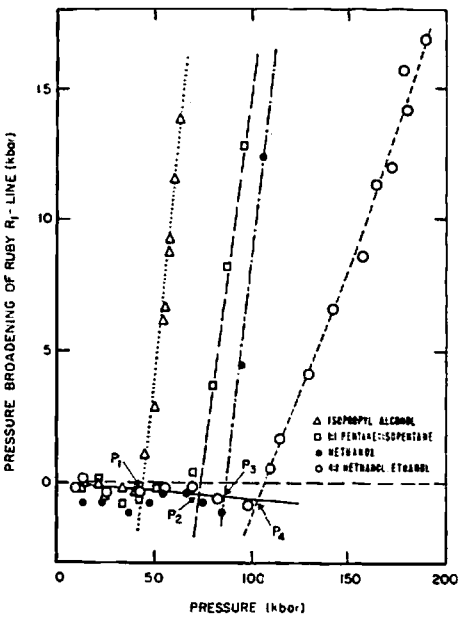

Fig. 11. Pressure broadening of the sharp ruby R_1 fluorescence line relative to the 1 atm linewidth for various pressure-transmitting liquids. The letter P with a numeral subscript represents the glass transition pressure for the given liquid. (10 kbar=1 GPa)

shall explain later, glass transition pressures can be predicted reliably from viscosity data by means of a critical point model.

Absolute viscosity is calculated using a modified Stokes equation:

$$\eta=[2a^2g(\rho-\rho_0)/9v]\gamma, \qquad (1)$$

where η=absolute viscosity (poise)
a=radius of sphere (cm)
g=acceleration due to gravity (cm s^{-2})
v=terminal velocity of sphere in liquid (cm s^{-1})
ρ=density of sphere (g cm^{-3})
ρ_0=density of liquid (g cm^{-3}), and
γ=a geometrical correction factor.

To be able to calculate accurate viscosities at pressure, the pressure dependence of v, ρ, and ρ_0 must be known as well as γ, the geometrical correction factor due to the wall effect. For a medium of infinite extent, the ideal Stokes limit, γ is unity. However, in the real case of a diamond cell there is an appreciable wall effect which must be well characterized in order to obtain accurate values of viscosity. We have examined this problem and have determined a multiplicative geometrical correction factor for the specific cell geometry of the DAPC.[39]

The physical reasoning that has been utilized is straightforward. Consider a right circular

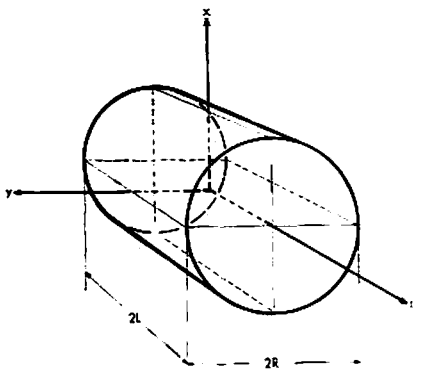

Fig. 12. Geometry and Cartesian axes for the diamond-anvil pressure cell. The figure is a cylinder of length $2L$ having a circular cross-section of diameter $2R$. The origin of the axes is at the center of the cylinder.

cylinder with a circular radius R and a length $2L$. (See Fig. 12) In the diamond cell configuration, a sphere of radius a falls along a diameter of the circular cross-section (along the x-axis in Fig. 12). The wall factor γ clearly must have the following characteristics:

$$\frac{d\gamma}{d(a/L)}<0 \text{ at constant } R/L. \tag{2}$$

This relation simply means that as the walls are removed to greater distances from the sphere, the wall effect must diminish.

$$\frac{d^2\gamma}{d(a/L)^2}\geq 0 \text{ at constant } R/L. \tag{3}$$

The relation (3) means that as the walls are removed to greater distances from the sphere, each successive step becomes less significant.

In addition to relations (2) and (3), the "boundary conditions" that $\gamma=1$ for an infinite volume and $\gamma=0$ when the walls come into contact with the sphere must be imposed. It follows directly that

$$\lim_{(R/L)\to\infty}\gamma(a/L,\ R/L)\leq 1-a/L \text{ for } 0\leq a/L\leq 1. \tag{4}$$

Relations for the variation of γ with respect to (R/L) can be obtained by similar reasoning.

$$\frac{d\gamma}{d(R/L)}>0 \text{ at constant } a/L. \tag{5}$$

$$\frac{d^2\gamma}{d(R/L)^2}\leq 0 \text{ at constant } a/L. \tag{6}$$

Proceeding from relations (2)—(6) and utilizing the exact results which can be obtained for concentric spheres, we have found the wall factor to be given as in Fig. 13.

To determine the viscosity according to Eq. (1), the terminal velocity of the falling sphere must be measured. This is achieved by monitoring the time interval that is required for the sphere to transverse a given distance. Ideally, the time increment per interval should

vary with position in the cell as shown in Fig. 14. The actual experimental behavior can be quite close to this as shown in Fig. 15.

The accuracy of the overall method has been examined by performing measurements on a liquid of known viscosity. Since the wall effect is dependent on the relative dimensions of the

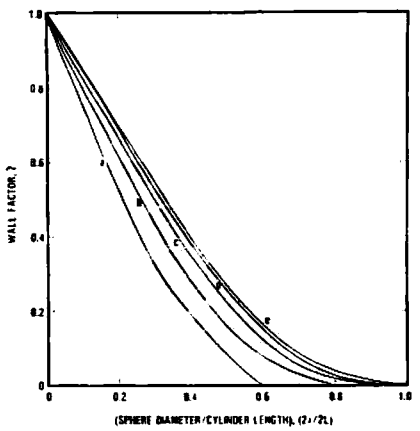

Fig. 13. Dimensionless wall factor γ for a right circular cylindrical viscometer of length $2L$ and radius R in which a sphere of radius a falls along a centrally located diameter. Curve a, $R/L=0.6$, curve b, $R/L=0.8$, curve c, $R/L=1.0$, curve d, $R/L=1.2$, curve e, $R/L=1.4$.

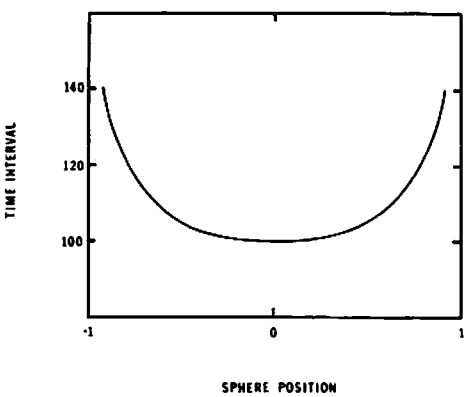

Fig. 14. Idealized graph of the time interval required for a sphere to travel one measuring unit of length at a normalized position in the diamond anvil cell. Arbitrary units are used here.

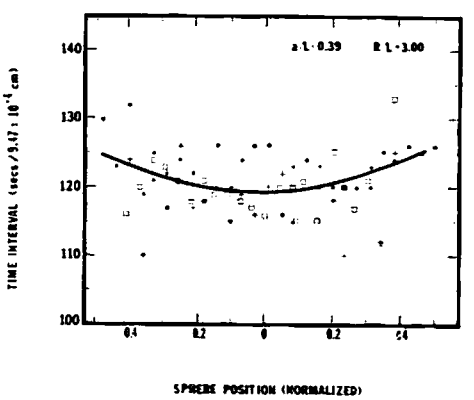

Fig. 15. Central portion of time intervals per measuring unit in (s/9.47×10⁻⁴ cm) *versus* normalized sphere position. The center of the cell occurs at position 0 and the boundaries occur at ±1. The solid curve is a least-squares parabola. $2a=0.066$ mm, $2L=0.169$ mm, and $2R=0.507$ mm. Dow-Corning fluid No. 200 is used.

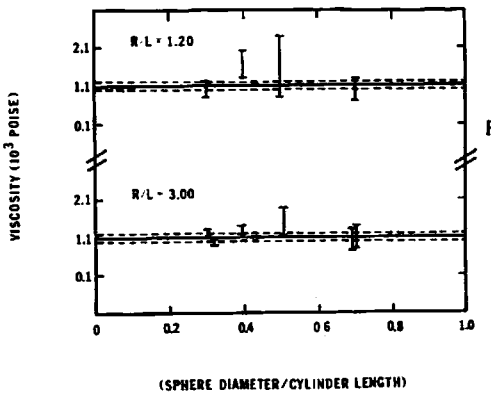

Fig. 16. Viscosity of Dow-Corning fluid No. 200 at room temperature and atmospheric pressure as measured in a diamond anvil cell. The solid and dashed lines show the known value of the viscosity and its uncertainty.

system, the viscosity determination was repeated for several cases as shown in Fig. 16. Since the initial work, the measurement system has been refined, and it is now estimated that the absolute viscosity can be determined with an accuracy of $\pm 10\%$.

The first substance studied with this system was 4:1 (by volume) methanol: ethanol, and the results obtained in that work are shown in Fig. 17. In this case, the viscosity was measured up to a pressure of 7.0 GPa (70 kbar). At that pressure, several days were required for one measurement point. Since the relationship between viscosity and pressure is at least exponential, the time required for one measurement point at 8.0 GPa would be on the order of 2×10^4 days. Thus, viscosity measurements above about 10^6 poise were impractical.

According to the ruby line broadening method, the glass transition pressure for 4:1 methanol: ethanol is about 10.4 GPa (see Fig. 11). As a first check on this value the curve shown in Fig. 17 was continued smoothly to a value of 10^{13} poise-the value generally associated with the onset of the glassy state. The smooth curve indicates that 10.4 GPa is not an

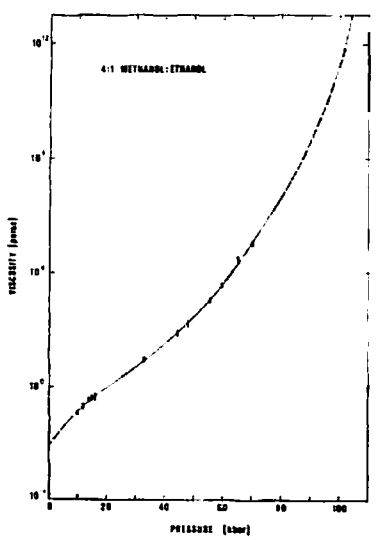

Fig. 17. The pressure dependence of the viscosity of a mixture of 4:1 (by volume) of methanol: ethanol at room temperature. The dashed lines are extrapolations to the glass transition (10^{13} poise) and to the viscosity of methanol at 1 atm (6×10^{-3} poise). (10 kbar = 1 GPa)

The Review of Physical Chemistry of Japan Vol. 50 (1980)

unreasonable value for the glass transition as a first approximation. However, the correlation between the glass transition pressure and the measured pressure dependence of viscosity needed to be put on a much more quantitative basis. As mentioned in the introduction, an examination of the literature revealed a considerable amount of uncertainty in this area with at least 30 empirical expressions for the temperature and pressure dependences of viscosity. Complicating this are several theories of the liquid state which include the free volume theory, the lattice model theories and the significant structure theory. Although each theory has been applied successfully in specific applications none has achieved universal success. Moreover, for the purpose of the present application, none of these theories permits a straightforward determination of the glass transition pressure. Consequently, we chose to follow an operational procedure that encompasses the general features for which there is agreement.

Several general features relevant to this problem are listed below.

(1) Vitrification is similar to a second-order phase transition.

(2) As the vitreous state is approached, there is increasingly cooperative-like-behavior among the particles.

(3) The pressure-dependence of viscosity increases faster than exponentially, slowly at pressures far removed from the glass transition and then rapidly over a small pressure range near the glass transition.

(4) The ratio of the viscosity at the glass transition pressure to the viscosity at one-half that pressure can be as large as 10^{10}.

These four features can be summarized by the statement "Near the glass transition, viscosity exhibits a nearly critical point behavior". The use of the words "critical point" is intended in the sense of a mathematical singularity. We consider, in other words, an expression of the type found in critical point phenomena:

$$\eta = A(1 - P/P_G)^{-\nu}, \tag{7}$$

where P_G is the glass transition pressure and ν is the critical exponent which determines the rate of change of viscosity. The qualitative features of this expression are in accord with the features we have noted for viscosity as demonstrated in Fig. 17. Therefore, the expression provides a reasonable analytical model which permits a straightforward evaluation of the glass transition pressure by means of a nonlinear least squares fit of this expression to the measured viscosity. We have done this for three cases for which high pressure viscosity data are available.

The experimental results for 4:1 methanol-ethanol are given in Figs. 11 and 17. As a further example, Figs. 18 and 19 give the results for *n*-butyl chloride. In Table 1, the values of the glass transition pressure obtained by the ruby line broadening measurements and by means of Eq (7) are compared. The agreement obtained in all three cases is satisfactory, especially when you consider that the results were obtained by two methods based on quite different and independent reasoning. Thus, we have two methods for determining glass

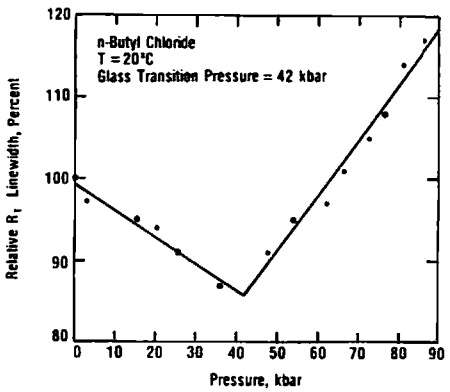

Fig. 18. Relative linewidth of the ruby R_1 fluorescence line as a function of pressure when *n*-butyl chloride is used as the pressure transmitting medium. The break point at 42 kbar is interpreted as the glass transition point.

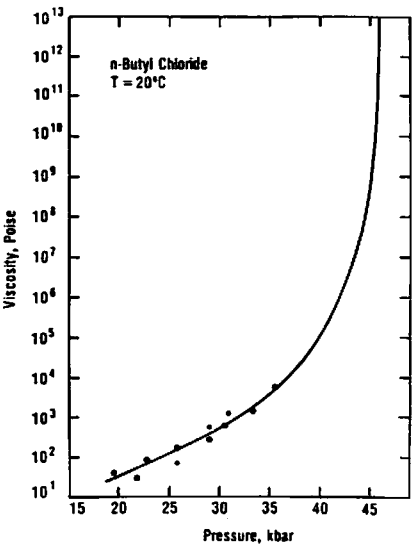

Fig. 19. Viscosity of liquid *n*-butyl chloride as a function of pressure at 20°C. The equilibrium freezing pressure is 23 kbars. Above 23 kbars, the liquid is metastable. The smooth curve is obtained from the analytic model discussed in section 4.

Table 1. Glass transition pressure P_t in GPa at T=20°C for 4 : 1 methanol-ethanol (4 : 1), metastable normal butyl chloride (NBC), and isopropyl alcohol (IA). The column labeled "linewidth" gives the values obtained by the ruby, R_1 line broadening method. The columns labeled "viscosity model" give the parameter values deduced from a least squares fit of the model of section 4 to the viscosity as a function of pressure

	Linewidth	Viscosity Model	
	P_t	P_t	ν
4 : 1	10.4	10.2	12.5
NBC	4.2	4.6	5.9
IA	4.5	5.1	18

transition pressures involving the use of different experimental data.

Beyond the agreement found for the two methods of determining the glass transition pressure, the viscosity model has a feature, the critical exponent, ν, which permits an evaluation of the rate of change of viscosity with pressure. This rate is determined by the molecular structure and the intermolecular bonding capability of the liquid. Thus, liquids that are similar in these respects should have comparable values of ν. Consequently, the exponent could be useful in classifying viscous liquids, and, in particular, it could provide a useful new piece of information for describing the properties of lubricants. Especially important would be the rate at which the glass transition is approached because under conditions of widely varying stresses, the rate parameter could be a very important consideration in evaluating the ability of a lubricant to respond satisfactorily to the changes in the stresses.

References

1) J. E. Lennard-Jones, *Proc. Roy. Soc.*, (*Lon.*), A106, 441 (1924).
2) T. G. Flox and P. J. Fory, *J. Appl. Phys.*, 21, 581 (1950).
3) M. L. William, R. F. Landell, and J. D. Ferry, *J. Amer. Chem. Soc.*, 77, 3701 (1955).
4) M. H. Cohen and D. Turnbull, *J. Chem. Phys.*, 31, 1164 (1959).
5) M. H. Cohen and G. S. Grest, *Phys. Rev.*, B20, 1077 (1979).
6) J. H. Gibbs and E. A. DiMarzio, *J. Chem. Phys.*, 28, 373 (1958).
7) G. Adams and J. H. Gibbs, *ibid* 43, 139 (1965).
8) I. C. Sanchez, *J. Appl. Phys.*, 45, 4204 (1974).
9) H. Eyring, T. Ree, and N. Hirai, *Proc. Nat. Acad. Sci.*, (*U. S.*) 44, 683 (1958).
10) H. Eyring and M. S. Jhon, "Significant Liquid Structures", Wiley New York (1969).
11) S. M. Breitling and H. Eyring, "Liquid Metals" (S. Z. Beer, editor). Marcel Dekker, Inc., (1972), Chap. 5.
12) J. P. Valleau, *Mol. Phys.*, 1, 63 (1959).
13) D. Chandler, *J. Chem. Phys.*, 62, 1358 (1975).
14) J. H. Dymond, *Chem. Phys.*, 17, 101 (1976).
15) H. C. Lonquet-Higgins and J. P. Valleau, *Mol. Phys.* 1, 284 (1959).
16) H. T. Davis, S. A. Rice, and J. V. Sengers, *J. Chem. Phys.*, 35, 2210 (1961).
17) H. T. Davis and K. D. Luks, *J. Phys. Chem.*, 69, 869 (1965).
18) W. C. Roentgen, *Wied. Ann.*, 22, 510 (1884).
19) C. Barus, *Am. J. Sci.*, 45, 87 (1893).
20) E. Kuss, *High Temp.-High Pressures*, 9, 415 (1977).
21) Y. Tanaka, T. Yamamoto, Y. Satomi, H. Kubota, and T. Makita, *Rev. Phys. Chem. Jpn.* 47, 12. (1977).
22) H. Kubota, S. Tsuda, M. Murata, T. Yamamoto, Y. Tankaka, and T. Makita, *ibid.*, 49, 59 (1979).
23) J. F. Hutton and M. C. Phillips, *Nature* (*Phys. Sci.*), 245, 15 (1973).
24) A. F. Collings and E. McLaughlin, *Trans. Faraday. Soc.*, 67, 340 (1971).
25) E. Dickinson, *J. Phys. Chem.*, 81, 2108 (1977).
26) P. W. Bridgman, *Proc. Am. Acad. Arts Sci.* 61, 57 (1926).
27) J. B. Irving and A. J. Barlow, *J. Phys.* E4, 232 (1971).
28) P. W. Bridgman, *Proc. Am. Acad. Arts. Sci.*, 77, 115 (1949).
29) V. Ziblerstein and J. Dill, Technical report number AFAPL-TR-78-73 (1978), Air Force Aero Propulsion Lab., Wright-Patterson Air Force Base, Ohio 45433.
30) I. Kushiro, *J. Geophys. Res.*, 81, 6347 (1976).
31) I. Kushiro, *Earth Planet Sci. Lett.*, 41, 87 (1978).

32) J. D. Barnett and C. D. Bosco, *J. Appl. Phys.*, **40**, 3144 (1969).
33) G. J. Piermarini, R. A. Forman, and S. Block, *Rev. Sci. Instrum.*, **49**, 1061 (1978).
34) S. Block and G. Piermarini, *Phys. Today*, **29**, Sept. 1976.
35) G. J. Piermarini and S. Block, *Rev. Sci. Instrum.*, **46**, 973 (1975).
36) J. D. Barnett, S. Block, and G. J. Piermarini, *ibid.*, **44**, 1 (1973).
37) G. J. Piermarini, S. Block, J. D. Barnett, and R. A. Forman, *J. Appl. Phys.*, **46**, 2774 (1975).
38) G. J. Piermarini, S. Block, and J. D. Barnett, *ibid.*, **44**, 5377 (1973).
39) R. G. Munro, G. J. Piermarini, and S. Block, *ibid.*, **50**, 3180 (1979).
40) R. G. Munro, S. Block, and G. J. Piermarini, *ibid.*, **50**, 6779 (1979).

Center for Materials Science
National Bureau of Standards
Washington, D. C. 20234
U. S. A.